Characterization of sugar alcohols as seasonal heat storage media - experimental and theoretical investigations

Document status and date:
Published: 01/01/2014

Document Version:
Publisher's PDF, also known as Version of Record (includes final page, issue and volume numbers)

Please check the document version of this publication:

• A submitted manuscript is the version of the article upon submission and before peer-review. There can be important differences between the submitted version and the official published version of record. People interested in the research are advised to contact the author for the final version of the publication, or visit the DOI to the publisher's website.
• The final author version and the galley proof are versions of the publication after peer review.
• The final published version features the final layout of the paper including the volume, issue and page numbers.

Link to publication

Characterization of sugar alcohols as seasonal heat storage media – experimental and theoretical investigations

Huaichen Zhang[1], Roel M. J. van Wissen[1] Silvia V. Nedea[1], Camilo C.M. Rindt[1]

[1]Department of Mechanical Engineering, Eindhoven University of Technology, Den Dolech 2, 5612AZ Eindhoven, Netherlands, Phone: +31-40-2473172, e-mail: h.zhang@tue.nl

Abstract

Sugar alcohols are under investigation as phase change materials for long term heat storage applications. The thermal performance in such systems is strongly dominated by the nucleation and crystal growth kinetics, which is further linked to the crystal-melt interfacial free energy (surface tension), the latent heat, and the viscosity. We carry out a comprehensive study of sugar alcohols to examine their thermodynamic and kinetic properties, from both experiments and theoretical calculations. The theoretical study follows a bottom-up approach. A generalized AMBER force field obtained from first principle calculations is selected to construct the molecular models. Heat capacity, self-diffusion constant, viscosity, latent heat, and interfacial free energy of selected model materials are calculated through molecular dynamic simulations. In the experimental study, differential scanning calorimetry and viscosity measurements are performed. Also, the kinetics of the crystal growth is examined using a microscope. The experimental results are integrated with the Rozmanov model, and a strong dependence of growth speed on the degree of subcooling is identified. All the experimental measurements are compared with our theoretical work, and the results showed good agreement. The methodologies used in the calculation are proved effective and reliable for future prediction of unknown systems. In this study, the high viscosity and the high interfacial free energy are both found responsible for the sluggish kinetics of nucleation and crystal growth in sugar alcohols.

Keywords: molecular simulation, sugar alcohols, nucleation and crystallization, phase transition

1. Introduction

Phase change materials have been extensively used in many industrial and residential applications. One such application involves storing solar heat in summer in order to cut down the energy consumption in the built environment in winter. Recent studies suggest using pure sugar alcohols (C4-C6 polyols) or their eutectic mixtures as seasonal heat storage media [1]. These materials have relatively high latent heat, proper melting temperatures for residential heating, and an evident subcooling effect for low-cost storage at ambient temperature. Besides, the vast availability and the low environmental impact make sugar alcohols good candidates for large-scale applications. Nevertheless, during preliminary studies, some drawbacks were identified. The thermal properties of these materials are not fully known, at least for the storage conditions. The degradation and cycling effect of the materials should be quantified to aid the storage system design. The low nucleation rate and unpredictable growth pattern hinder the heat transfer process, resulting in low and poorly controlled discharge power. All these difficulties make it indispensable to have a full investigation of these materials, including their thermodynamic and

transport properties, from both experimental and theoretical approaches. These properties include specific heat capacity, latent heat of fusion, melting point, shear viscosity, growth speed of crystal front, and crystal-melt interfacial free energy. These properties are essential for the design of storage reactors, in terms of optimal operating temperature, storage capacity, discharge power and the mechanical structures. It is known that sugar alcohols suffer from thermal degradation if exposed to high temperature. It is therefore our task to also quantify the effect of thermal degradation on the storage capacities of the model materials. The bottom-up theoretical approach provides in-depth understandings about the physics and reliable predictions whenever experiments are not applicable. In this work, erythritol, adonitol, D-mannitol, and xylitol are selected for investigation, all of which are found to be potentially the best candidates of seasonal heat storage [1]. The thermal properties and shear viscosity measurements are unified by Rozmanov model [2] in the crystal growth speed measurements. All experimental facts are backed up by our theoretical calculations which in turn proved our theoretical model. In this paper, we will first give a description of both experimental and simulation methods. Then the results are compared and discussed before the conclusions are drawn.

2. Material and experimental method

2.1 Materials

Meso-erythritol (Sigma, CAS 149-32-6, >99% pure), adonitol (Sigma, CAS 488-81-3, >99% pure), D-mannitol (Sigma-Aldrich, CAS 69-65-8, >98% pure), xylitol (Sigma, CAS 87-99-0, >99% pure) are used in the experiments. These materials are shipped in granular shape with diameters ranging from 0.1 to 1.0 mm.

2.2 Thermal analysis

Thermal analysis was used to obtain the melting temperature T_m, the latent heat of fusion ΔH_m, the specific heat capacity c_p of selected sugar alcohols. In this work, these thermal properties are measured using differential scanning calorimetry (DSC). In DSC, the change of heat (enthalpy) as a function of temperature or time is measured when the sample is subjected to a preset uniform rate of change in temperature.

The DSC measurements are carried out in the Materials and Interface Chemistry Laboratory in Eindhoven University of Technology (Eindhoven, the Netherlands). The apparatus used is the TA Instruments Q2000 model, which is calibrated via an indium calibration. The data calibration rate is set to 600 Hz and the rate of change in temperature is set to 10 K/min. The sample sizes are around 10mg. Sugar alcohols can degrade when exposed to high temperature. The thermal performances of degraded sugar alcohols are much lower than the new materials. To avoid degradation, the first cycle of measurement is made to determine the melting temperatures. In the measurements of c_p and ΔH_m, the maximum heating temperature is set to $T_m + 10K$.

To further examine the influence of degradation, all samples are exposed to $T_m + 40K$ for two hours. T_m and ΔH_m of the degraded sugar alcohols are then measured to study the changes in the thermal performances.

2.3 Rheology

Shear viscosities μ of the model sugar alcohols are measured using a TA instruments ARES rheometer. The rheometer is calibrated with oil at 23 °C and gives 10.7 Pa·s and 4% relative error as compared with the reference. The error is assessed to be accurate enough to perform the viscosity measurements. Before the measurements, a dynamical mechanical analysis is made for all the materials. The shear frequency of the viscometer is set to vary from 0.1 Hz to 100 Hz with 20 measurement points for each sugar alcohol. In all the experiments, the shear viscosity

modulus remains constant, indicating all these sugar alcohols are good Newtonian fluids in the selected shear frequency range.

The viscosities are then measured for a range of temperatures. The initial temperatures are around $T_m + 5K$. The cooling rates are fixed at 1.85 K/min and viscosity data are taken every 2.2 s. When phase change occurs, the rheometer gives an overload error, and the measurement automatically stops.

2.4 Crystal growth measurements

The crystal growth kinetics are directly linked to the heat power and thermal performances of the heat storage system. The growth rates are measured using an optical microscope with a camera recording real-time images. The experimental setup is demonstrated in Figure 1. The liquid sample of around 500 mg is placed on top of a heating platform controlled by a feedback controller. To initiate crystal growth, small grains that act as seeds are placed in the liquid sample before the image acquisitions. The mass of these grains is less than 0.5 mg.

From the recorded images, the growth speed of the crystal frontiers can be determined in the unit of µm/s. It is difficult to track the growth speed of each crystal facet. Therefore, the growth speed of the frontier is assumed to be an averaged isotropic value of growth speed. This is a reasonable assumption because the high surface nucleation rate and the growth that follows can quickly fill in the gaps between dendrites resulting in a spherical crystal on a larger scale.
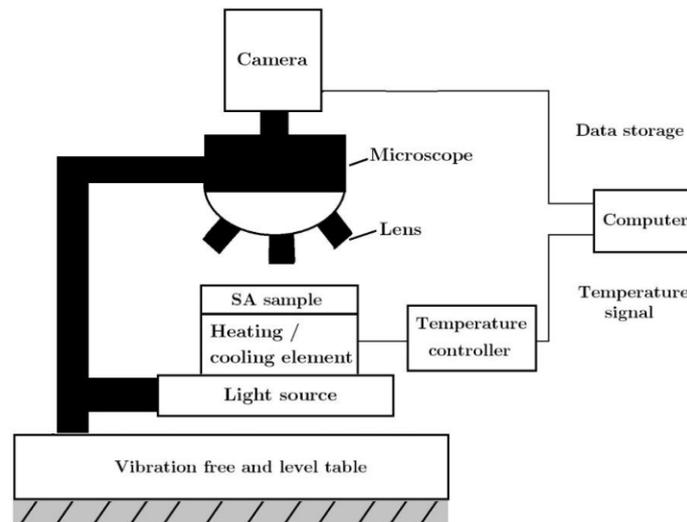

Figure 1. Experimental setup for crystal growth speed measurements.

The growth speed is measured at different degrees of subcooling for adonitol, xylitol, D-mannitol and erythritol. The temperature dependent growth speed is then fit by a theoretical model discribed by Rozmannov [2], which adopts the following form,

$$R(T) = C_1 e^{C_2/T} \sqrt{D(T)} \left[1 - C_3 e^{C_4/T} \right] \tag{1}$$

where R is the growth speed, D is the self-diffusivity, C1, C2, C3, and C4 are thermodynamic parameters fitted from the growth experiments or computed from other known thermodynamic parameters. Here, we take

$$C_3 = e^{\Delta H_m/RT}, \; C_4 = -\Delta H_m / R \tag{2}$$

and fit only C_1 and C_2. R is the gas constant 8.314 JK^{-1}mol^{-1}. The self-diffusivity is computed from the measured temperature-dependent shear viscosity by the Stokes-Einstein relation [3]

$$D(T) = \frac{k_B T}{6\pi\mu(T)r_h} \tag{3}$$

where k_B is the Boltzmann constant and r_h is the hydrodynamic radius. r_h can be calculated from the liquid density assuming a dense spherical packing using

$$\frac{4\pi r_h^3}{3p}\rho(T) = \frac{M}{N_A} \tag{4}$$

where p is the packing fraction 0.74048, M is molar mass [kg/mol], ρ is temperature dependent density, N_A is Avogadro's number.

3. Molecular modeling method

3.1 Molecular model

The molecular model is made from a generalized AMBER force field [4]. The force field is tailored to match quantum chemical calculations and can reliably provide the physical details of the molecules. In this full-atom force field, every atom is modeled explicitly, with a set of conservative potentials governing the exact motions of every atom in the molecular liquids. The potential can be expressed as

$$E_p(\mathbf{r}_1,\mathbf{r}_2,\ldots,\mathbf{r}_N) = E_{bond} + E_{angle} + E_{dih} + E_{LJ} + E_{el} \tag{5}$$

where the energy terms represent total potential energy, bond stretching energy, angle bending energy, dihedral rotation energy, van der Waals interaction with Lennard-Jones form, and electrostatic interaction, respectively. $\mathbf{r}_i$ represent the vectors of each atom in the system. More details are given in [4].

The above molecular model is used in our molecular dynamics simulations. In the simulations, initial configurations are generated either directly from crystallographic data or from equilibration simulations under certain temperature and pressure conditions. In each iteration, the potential energy is calculated using equation (5) based on the instantaneous configuration ($\mathbf{r}_1$, $\mathbf{r}_2,\ldots$, $\mathbf{r}_N$). Then the forces are calculated using $\mathbf{F} = -\nabla E_p$. These forces act on every atom in the system following the Newton's equations of motion, and a new configuration is generated as the input for the next iteration. In this manner, a time-evolving trajectory is formed and this trajectory can then be used to calculate the thermodynamic or kinetic properties of the system.

3.2 Heat of fusion and specific heat capacity

In the theoretical work of molecular modeling, the enthalpy-temperature curve is generated by heating up the molecular crystals by a constant heating rate at a fixed atmospheric pressure. The classic enthalpies H_{CL} are directly measured from the simulations. However, because of the classic nature of the molecular simulations, the enthalpies should be corrected using the normal mode analyses presented in the following equation, assuming all atoms are harmonic quantum oscillators [5].

$$H_{QM} = H_{CL} + k_B T \sum_{i=1}^{3N-3}\left(\frac{1}{2}x_i - 1 + \frac{x_i}{e^{x_i}-1}\right) \tag{6}$$

where H_{QM} is the corrected enthalpy using quantum oscillators instead of classical oscillators, $x_i = h\nu_i / k_B T$, h is the Planck constant, ν_i are the eigen frequencies from normal mode analyses of the system. The specific heat capacity is then defined as the derivative of enthalpy over temperature.

The specific heat of fusion ΔH_m is defined as the enthalpy difference between the crystal and melt phases at the melting point.

3.3 Self-diffusivity and shear viscosity

The self-diffusion constants D are calculated based on the Einstein relation

$$\lim_{t \to \infty} \left\langle \left\| \mathbf{r}_i(t) - \mathbf{r}_i(0) \right\|^2 \right\rangle_i = 6Dt \tag{7}$$

where $\mathbf{r}$ is atomic coordinate vector, t is time, $\langle \ \rangle_i$ denotes ensemble average over all atoms i in the system. In the simulations, the molecular fluids are prepared by melting the solids and then equilibrating at various temperatures. Then the mean squared displacements (the expression inside the angle brackets in equation (7)) are calculated and used for obtaining self-diffusion constants.

The shear viscosities are obtained using Stokes-Einstein relation in equation (3). The hydro-dynamic radii are calculated using equation (4).

3.4 Interfacial free energy

Interfacial free energy controls the rate of nucleation. In the theoretical study, the interfacial free energies are estimated using the superheating-undercooling hysteresis method (SUH) [6]. In this method, molecular crystals are heated with various heat rates. Based on the observed melting temperature T_+ (which is above the static melting point T_m), the interfacial free energy γ_{SL} can be estimated using the following equations

$$\gamma_{SL} = \left(\frac{3}{16\pi} \beta k_B T_m \Delta H_{m,V}^2 \right)^{1/3} \tag{8}$$

$$\beta = \left(59.4 - 2.33 \log_{10} Q \right) \frac{T_+}{T_m} \left(\frac{T_+}{T_m} - 1 \right)^2 \tag{9}$$

where Q is the heating rate in the unit K/s, $\Delta H_{m,V}^2$ is volumetric heat of fusion. In the calculations, $\Delta H_{m,V}$ and T_m are experimental values.

3.5 Simulation details

All molecular simulations are performed using the GROMACS-4.5.5 package [7]. The molecular crystal systems (configurations) are constructed by replicating unit cells obtained from experimental crystallographic data [8,9]. The cuboid simulation boxes have a typical side length of 4-5 nm. The temperatures and pressures are controlled by Berendsen thermostat and barostat [10]. The time step of each iteration is set to 2 fs, and the simulations last for 100 to 500 ps for energy and diffusion calculations. The simulation lengths for SUH simulations vary from 1 to 10 ns dependent on the heat rate settings.

4. Results and discussions

4.1 Thermal analysis

The specific heat capacities c_p for both solid and liquid (including subcooled liquid) are measured and fitted by quadratic functions of temperature in [°C] in the form of $c_p(T) = AT^2 + BT + C$. One such example is shown in figure 2. All fitted parameters are listed in table 1.
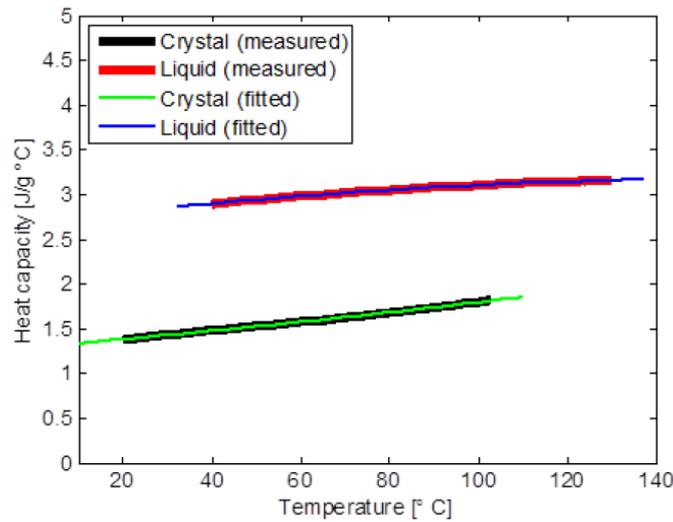
Figure 2. Measured and fitted c_p of erythritol by a quadratic function.

Table 1. Fitted parameters for all quadratic models describing the heat capacity

Polyol	A(95% confidence)	B (95% confidence)	C (95% confidence)	R²	Validity range
Erythritol (crystal)	$8.509 \cdot 10^{11}$ ($\pm 1.28 \cdot 10^{10}$)	$4.128 \cdot 10^{-3}$ ($\pm 1.4 \cdot 10^{-5}$)	1.303 (± 0.001)	0.9994	$20 < T < 110$
Erythritol (liquid)	$-1.741 \cdot 10^{-5}$ ($\pm 4. \cdot 10^{-8}$)	$5.88 \cdot 10^{-3}$ ($\pm 7.0 \cdot 10^{-6}$)	2.696 (± 0.001)	0.9999	$40 < T < 130$
Xylitol (crystal)	$-3.9 \cdot 10^{-6}$ ($\pm -5.36 \cdot 10^{-7}$)	$5.953 \cdot 10^{-3}$ ($\pm 5.6 \cdot 10^{-5}$)	1.267 (± 0.001)	0.9964	$20 < T < 85$
Xylitol (liquid)	$-2.345 \cdot 10^{-5}$ ($\pm 1.1 \cdot 10^{-7}$)	$6.547 \cdot 10^{-3}$ ($\pm 1.4 \cdot 10^{-5}$)	2.578 (± 0.001)	0.9995	$20 < T < 110$
Mannitol (crystal)	$1.244 \cdot 10^{-6}$ ($\pm 9.4 \cdot 10^{-8}$)	$4.83 \cdot 10^{-3}$ ($\pm 1.5 \cdot 10^{-5}$)	1.242 (± 0.001)	0.9993	$20 < T < 140$
Mannitol (liquid)	$-1.94 \cdot 10^{-6}$ ($\pm 1.43 \cdot 10^{-7}$)	$1.455 \cdot 10^{-3}$ ($\pm 1.4 \cdot 10^{-5}$)	3.101 (± 0.003)	0.9933	$110 < T < 170$
Adonitol (crystal)	$3.247 \cdot 10^{-5}$ ($\pm 4.5 \cdot 10^{-7}$)	$3.032 \cdot 10^{-3}$ ($\pm 4.2 \cdot 10^{-5}$)	1.113 (± 0.001)	0.9991	$20 < T < 75$
Adonitol (liquid)	$-2.516 \cdot 10^{-5}$ ($\pm 1.4 \cdot 10^{-7}$)	$6.16 \cdot 10^{-3}$ ($\pm 1.8 \cdot 10^{-5}$)	2.438 (± 0.001)	0.9984	$20 < T < 110$

After exposed to $T_m + 40K$ for two hours, the sugar alcohols degrade and become tanned. The thermal properties change during this process, specifically the latent heat of fusion. In the case of xylitol (figure 3), the melting process produces a milder peak and total amount of heat absorbed is reduced for the degraded sample. The effect of thermal degradation on T_m and ΔH_m are listed in table 2. The melting temperatures after degradation do not change much and are within the range of the heat flux peaks (figure 3). Erythritol and D-mannitol have the highest percentage of ΔH_m reduction during degradation. Note that they are also the materials with the highest ΔH_m.
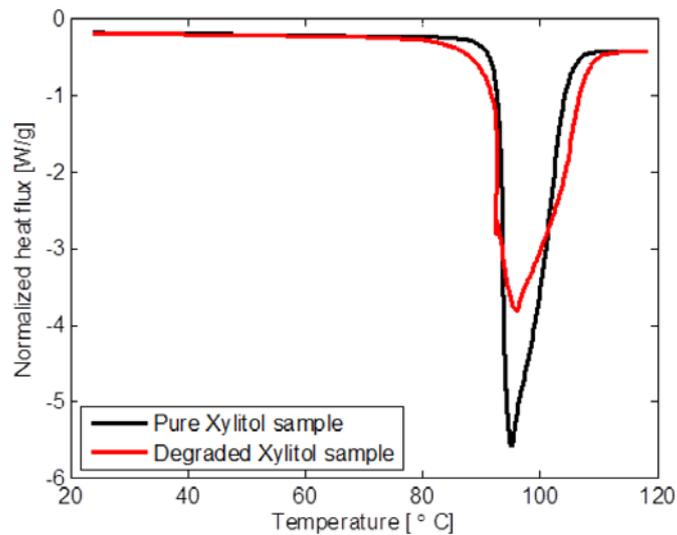
Figure 3. Heat flux peaks before and after thermal degradation of xylitol.

Table 2. Comparison of T_m and ΔH_m between pure and degraded sugar alcohols

Property	T_m [°C] (original)	T_m [°C] (degraded)	ΔH_m [kJ/kg] (original)	ΔH_m [kJ/kg] (degraded)	Percentage of ΔH_m reduction
Erythritol	119.4	114.3	338.7	271.6	19.8%
Xyliyol	95.1	96.0	251.4	231.7	7.8%
Adonitol	103.7	101.6	231.2	217.4	6.0%
D-mannitol	166.9	164.0	296.1	248.1	16.2%

The specific heat capacities of xylitol and α-D-mannitol are calculated using molecular simulations and normal mode analyses. There is a good agreement between theory and experiments, see figure 4. The experimental D-mannitol sample consists of a mixture of α, β, and δ form whereas the numerical sample represents the pure α form. Possibly this resulted in the small discrepancy between the experimental and numerical results as seen in figure 4(b). The liquid c_p is not calculated in this work. The measurement of liquid c_p coveres also the subcooled region. At the same temperature, the subcooled liquid has higher c_p than that of crystal. The measured liquid c_p of xylitol is slightly higher than that from [11]. The ΔH_m of xylitol from molecular modeling is 31.0 ±1.0 kJ/mol, which is lower than experimental values of 38.2 kJ/mol obtained in this work and 33.68 ± 0.34 kJ/mol from [11].
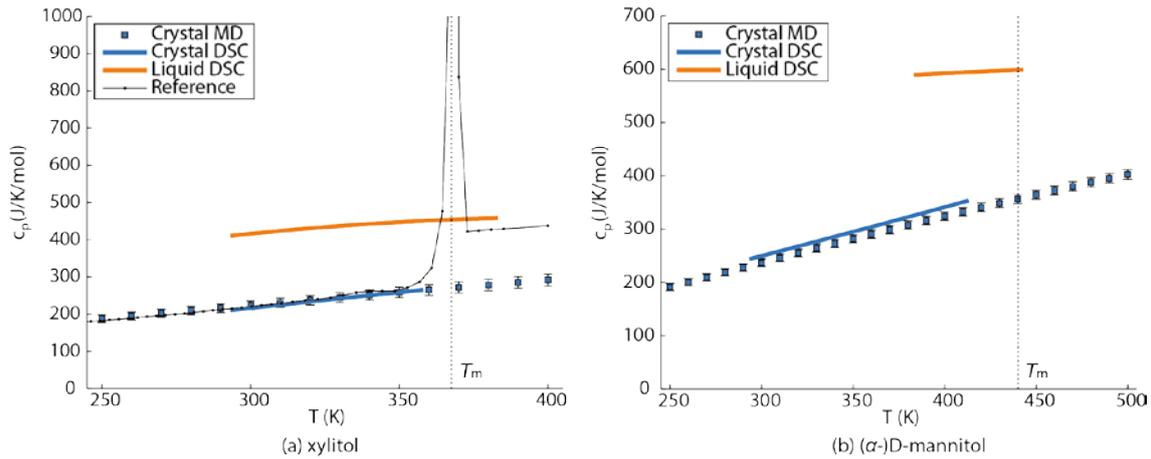
Figure 4. Predicted cp of crystalline (a) xylitol and (b) α-D-mannitol as compared with experimental measurements. The black dotted line in (a) is taken from reference [11].
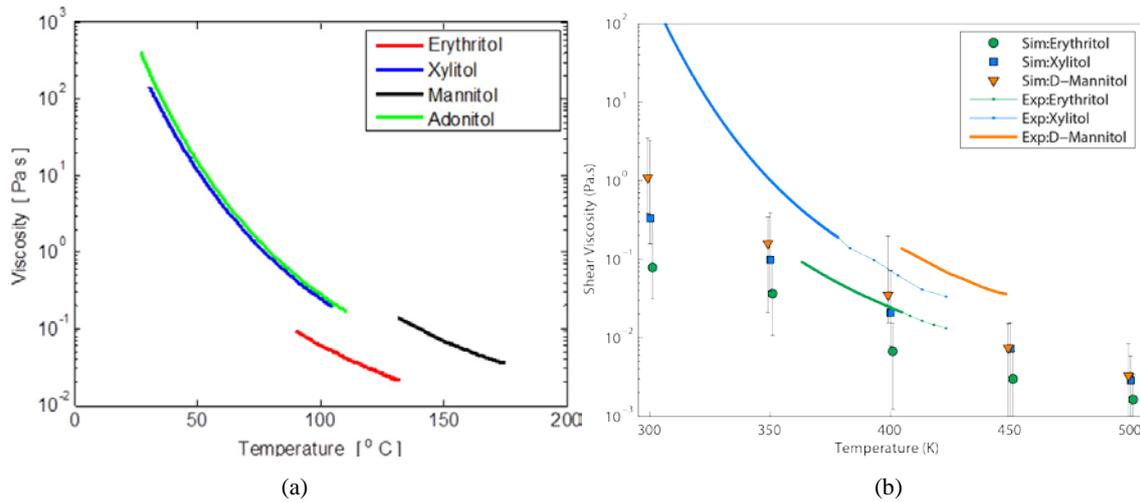
4.2 Shear viscosity

Figure 5. (a) Measured shear viscosities of selected model sugar alcohols and (b) A comparison between theoretical prediction and the measurements.

The key transport property that affect the kinetics of nucleation and crystal growth is the shear viscosity μ. The viscosity measurement results are shown in figure 5(a). It can be seen that viscosity is strongly dependent on temperature. This relationship is not limited to the thermally activated process, which states that μ is proportional to $\exp(G_\mu/k_B T)$, where G_μ is the activation free energy of viscous flow.

The theoretical prediction of μ is based on the self-diffusion coefficients D and Stokes-Einstein relations. The calculated results are shown in figure 5(b) with experimental results plotted as references. The self-diffusion constants D decrease with decreasing temperature and the shear viscosity μ increases with decreasing temperature. There is roughly a linear relationship between $\ln(\mu)$ and T from the simulation point of view. This matches the thermal activation interpretation aforementioned although the experiments suggest otherwise. The molecular models in all cases underestimate the shear viscosities.

4.3 Crystal growth measurements

The steady-state growth speed is measured directly from the microscopic images. Two examples are given in figure 6. In xylitol case, the growth speed is determined by a moving

frontier of a selected edge. The speed is not very sensitive to the selection of edges, as far as the edge roughly depicts the outline of the crystal. In D-mannitol case, the prismatic shaped growth is relatively rapid. Though anisotropic, the growth frontiers roughly forms a circle. Therefore, in this case the frontier is chosen as the circumference of the growing crystal.

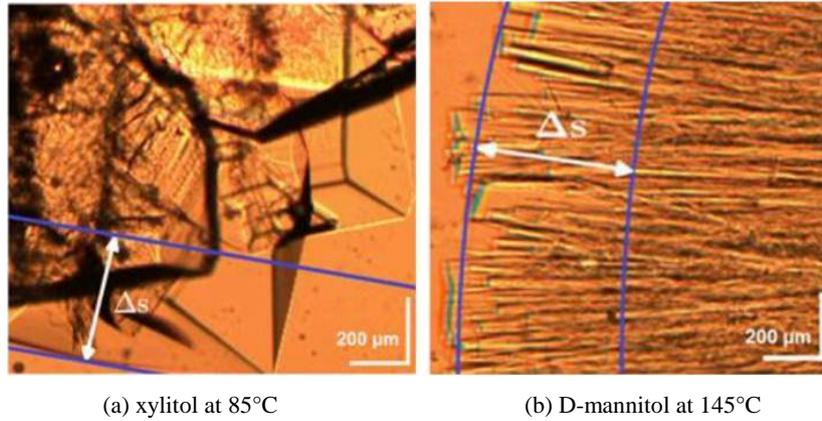| (a) xylitol at 85°C | (b) D-mannitol at 145°C |

Figure 6. Images taken in the crystal growth experiments of (a) xylitol and (b) D-mannitol. The growth speeds are determined from the distances of moving frontiers Δs over time interval Δt.

The measured growth speeds are plotted in figure 7 in black circles. In the xylitol and adonitol cases, there are clear peaks, below which the speeds decrease. The decrement is interpreted as the lack of mobility in the diffusion motions. In the theoretical study, the lack of mobility is quantified by the decreased self-diffusion constant. In the D-mannitol case, it is not clear whether the growth speed will decrease passing a maximum value because it is hard to achieve the subcooling required without spontaneous nucleation.
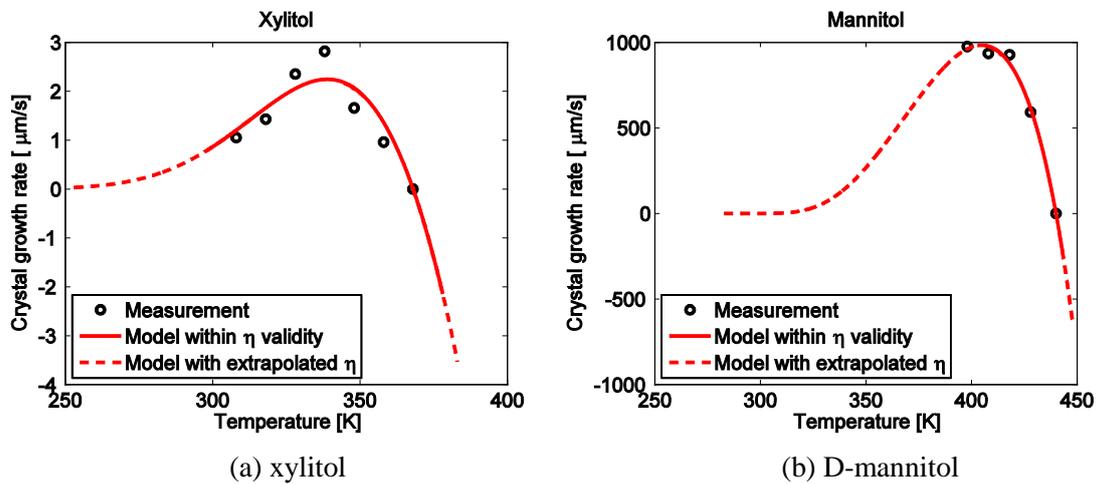

| (a) xylitol | (b) D-mannitol |

Figure 7. Measured crystal growth speed of (a) xylitol and (b) D-mannitol at various temperatures. The red lines are the fitted growth speed using Rozmannov model.

In all cases, the growth speeds are fitted by using equation (1). The theoretical model success-fully quantified the temperature dependent growth speeds. The dependence on temperature provides very important information on the reactor designs. To maximize the discharge power, the heat power should be controlled such that the storage media operates at an optimal temperature.

4.4 Interfacial free energy and nucleation rate

The solid-liquid interfacial free energy γ_{SL} is estimated from computer simulations. The observed superheated melting temperatures T_+ are labeled in Figure 8. With a higher heating rate, the phase transition happens at a higher temperature. In the limit of zero heating rate, T_+ will converge to the thermodynamic melting temperature T_m. In the calculations, $\Delta H_{m,V}$ and T_m are taken from the measured values in our thermal analysis. For xylitol, $\Delta H_{m,V} = 2.903 \times 10^8$ J/m^3, $T_m = 367.5$ K. For D-mannitol, $\Delta H_{m,V} = 4.595 \times 10^8$ J/m^3, $T_m = 438.0$K. For erythritol, $\Delta H_{m,V} = 4.760 \times 10^8$ J/m^3, $T_m = 391.0$K. The estimated γ_{SL} of xylitol is 58 mJ/m^2 and β-D-mannitol 78 mJ/m^2, 18 mJ/m^2 erythritol.

In the classical nucleation theory, the nucleation rate is proportional to exp(-ΔG^*/kT), where ΔG^* is the nucleation free energy barrier. At the same degree of subcooling, ΔG^* is proportional to $\gamma_{SL}^3 \, T_m^2/\Delta H_{m,V}^2$. Due to the accuracy of these calculations and the simplicity of the classical nucleation theory, it is inappropriate to provide detailed quantitative information on the nucleation rate. However, the free energy barrier of nucleation of erythritol is an order of magnitude smaller than that of xylitol and D-mannitol. This qualitative analysis can be used to explain why xylitol and D-mannitol can be stored at a large degree of subcooling without solidification while erythritol is very unstable at large degrees of subcooling.
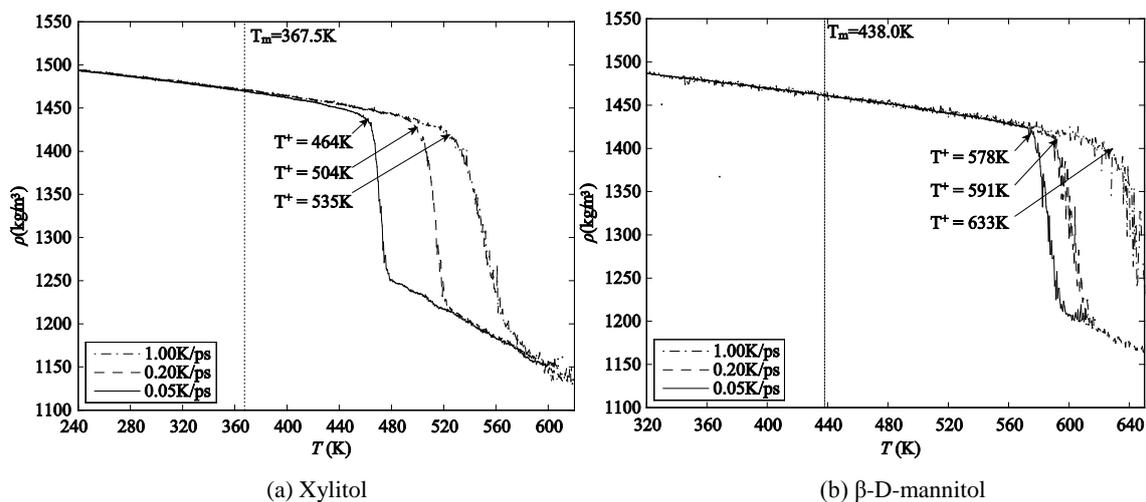

(a) Xylitol (b) β-D-mannitol

Figure 8. The density curves simulated by heating up crystalline (a) xylitol and (b) β-D-mannitol at various heating rates. The observed melting temperatures are lables as T$_+$.

5. Conclusions

A comprehensive study on the thermal properties and crystallization kinetics is carried out for a list of selected sugar alcohols which are most promising candidates for seasonal heat storage applications. In the experimental studies, we found that the latent heat of fusion evidently decreases after thermal degradation. Therefore, high temperature operation conditions should be avoided in the storage systems. Also, the crystal growth speed is found highly dependent on temperature. The rate of phase transition and discharge power of storage tanks are hence controlled by the operating temperature. The decrease in growth speed below the optimal point is caused by the dramatic decrease in self diffusivity. The measured thermal properties are well supported by our molecular modeling method. The calculated interfacial free energies for both xylitol and D-mannitol are relatively high and are probably related to the low nucleation rates and large subcooling effects in these systems.

Acknowledgements

References

[1] Elena Palomo del Barrio. SAM.SSA: Sugar alcohol based materials for seasonal storage applications. @Website: http://samssa.eu/, 2013.

[2] D. Rozmanov and P.G. Kusalik. Temperature dependence of crystal growth of hexagonal ice. *Physical Chemistry Chemical Physisc*,13:15501-15511, 2011.

[3] J.T. Edward. Molecular volumes and the Stokes-Einstein equation. *Journal of Chemical Education*, 47:261-270, Apr 1970.

[4] J. Wang, R.M. Wolf, J.W. Caldwell, P.A. Kollman, and D.A. Case. Development and testing of a general amber force field. *Journal of Computational Chemistry*, 25(9):1157–1174, 2004.

[5] D.A. McQuarrie. *Statistical mechanics*. New York: Harper & Row; 1976.

[6] S. Luo, T.J. Ahrens, T. Cagin, A. Strachan, W.A. Goddard, and D.C. Swift. Maximum superheating and undercooling: Systematics, molecular dynamics simulations, and dynamic experiments. *Phys. Rev. B*, 68:134206, Oct 2003.

[7] B. Hess, C. Kutzner, D. van der Spoel, and E. Lindahl. GROMACS 4: Algorithms for Highly Efficient, Load-Balanced, and Scalable Molecular Simulation. *J. Chem. Theory Comput.*, 4(3):435–447, Feb 2008

[8] A.Ø. Madsen, S. Mason, and S. Larsen. A neutron diffraction study of xylitol: derivation of mean square internal vibrations for H atoms from a rigid-body description. *Acta Crystallographica Section B*, 59(5):653–663, Oct 2003.

[9] F.R. Fronczek, Haidy Nasr Kamel, and Marc Slattery. Three polymorphs (α, β, and δ) of D-mannitol at 100K. *Acta Crystallographica Section C*, 59(10):o567–o570, Oct 2003.

[10] H.J.C. Berendsen, J.P.M. Postma,W.F van Gunsteren, A. DiNola, and J.R. Haak. Molecular dynamics with coupling to an external bath. *The Journal of chemical physics*, 81:3684, 1984.

[11] B. Tong, Z. Tan, Q. Shi, Y. Li, D. Yue, and S. Wang. Thermodynamic investigation of several natural polyols (I): Heat capacities and thermodynamic properties of xylitol. *Thermochinica Acta*, 457:20-26, 2007